Stack Plume Aerosol Retrieval from Prisma Hyperspectral Images

Gabriel Calassou, Pierre-Yves Foucher, Jean-Francois Leon

STACK PLUME AEROSOL RETRIEVAL FROM PRISMA HYPERSPECTRAL IMAGES

Gabriel Calassou[a], Pierre-Yves Foucher[a], Jean-François Léon[b]

[a]ONERA "The French Aerospace Lab", 2 Av. Edouard Belin, 31055 Toulouse, France
[b]Laboratoire d'Aérologie, Université Toulouse 3 Paul Sabatier, CNRS, Toulouse, France

ABSTRACT

In this paper, the physical and optical properties of aerosol plumes emitted by industrial stacks are analyzed using hyperspectral PRISMA satellite images. The plume aerosol optical thickness (AOT) and aerosol modal radius are retrieved with an algorithm using the statistical formalism of the optimal estimation method. SENTINEL-2/MSI data are also used to constrain the surface reflectances. The algorithm is applied to fine particle emissions from three industrial sites: a flaring emission from a gas flaring at an oil extraction site in Hassi Messaoud, Algeria (07/09/2021), a steel plant in Wuhan, China (03/24/2021) and a coal plant in Kendal, South Africa (09/25/2021). The mean fine mode radii vary between 0.10 to 0.39 μm, 0.30 to 0.70 μm and 0.40 to 1.25 μm for the flaring site, the steel site and the coal plant, respectively. These radii are associated with AOTs varying between 0.2 to 1.0 for the flare emission, 0.5 to 3.4 for the steel plant and 0.6 to 2.4 for the coal plant.

Index Terms— hyperspectral imagery, aerosols, stack emission

1. INTRODUCTION

Industrial stack emissions contribute significantly to the atmospheric particulate matter burden. According to the European Environmental Agency, the industrial sector has contributed to the PM_{10} and $PM_{2.5}$ emissions in Europe between 2013 and 2018 by 15% and 6.5%, respectively. Monitoring the contribution of stack emissions to the ambient PM_{10} or $PM_{2.5}$ requires a dense measurement network in the vicinity of the emitters and an accurate estimate of the channeled emission fluxes. Satellite imagery is a proven technique for stack plume detection although the quantitative retrieval of aerosol properties within the plume remains a challenge. We propose a new method to detect stack plume aerosol properties from hyperspectral satellite imagery.

2. DATA

PRISMA (PRecursore IperSpettrale della Missione Applicativa) is a medium-resolution hyperspectral imaging mission launched in 2019. PRISMA carries a camera with 239 spectral channels between 0.4 and 2.5 μm with a pixel resolution of 30 m.

Additionally to PRISMA data, SENTINEL-2/MSI observations within a few days delay from PRISMA acquisitions are used in the proposed method to better constrain the surface reflectance conditions over the targeted scenes. MSI has 13 spectral bands between 0.4 and 2.2 μm. The pixel resolution is between 10 and 60 m depending on the channel.

PRISMA and MSI images were acquired over three industrial complexes during the year 2021: a steel plant in Wuhan, China on March 24, a gas flaring at an oil extraction site in Hassi Messaoud, Algeria on July 9, and a coal-fired power plant in Kendal, South Africa on September 25. Stack plumes can be visually identified in the different color compositions (Figure 1).

3. METHOD

The method proposed by Calassou et al., (2021) [1] is applied to the PRISMA and MSI acquisitions. The method relies on a Bayesian approach following the formalism proposed by Rodgers. The state vector is composed of the plume fine mode modal radius r and the plume aerosol optical thickness (AOT) at 550 nm, τ_{550}. The uncertainties coming from the prior constraints and the observations are accounted for during the restitution of each of these parameters. The observations uncertainties S_ϵ are defined as the sum of the instrumental noise S_y and the uncertainties of the non-retrieved parameters b, ie. the water vapor concentration, the optical thickness of the background atmosphere and the surface reflectances.

The measurements are initially expressed in radiance L ($W{\cdot}m^{-2}{\cdot}sr^{-1}{\cdot}m^{-1}$). For convenience, we normalize the solar illumination by transforming the radiance L into a Top of Atmosphere (TOA) reflectance ρ_{TOA}. For a flat and Lambertian surface, ρ_{TOA} can be expressed as :

$$\rho_{TOA} = \left(L_{atm} + \rho \frac{(E_{sca} + E_{dir}) \times (T_{sca} + T_{dir})}{\pi(1 - \rho S)} \right) \times \frac{\pi}{E_{TOA}\mu_s}, \quad (1)$$

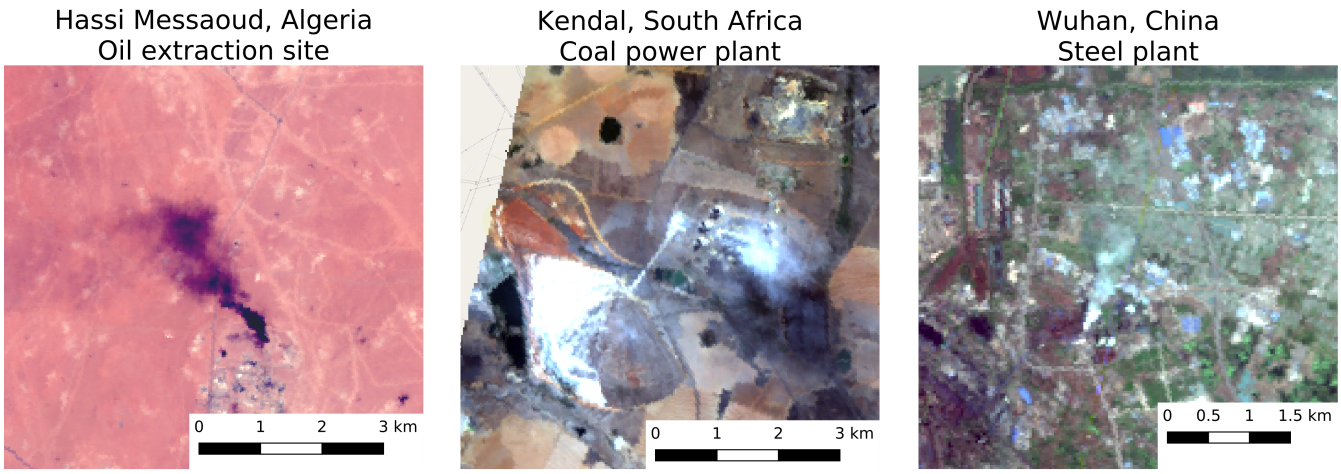

Fig. 1. PRISMA surface reflectance images of the gas flaring (left), a coal-fire plant (center) and a steel plant (right).

$L_{atm}$is the atmospheric radiance, ρ is the surface reflectance, E_{sca} and E_{dir} are respectively the scattering and the direct part of the downward solar irradiance received by the ground, T_{sca} and T_{dir} are the scattering and the direct upward transmittance and S the atmospheric spherical albedo. E_{TOA} is the TOA solar downward irradiance and μ_s the cosine of the solar zenith angle. The measurement vector y contains the measured TOA reflectance for each PRISMA wavelength outside the water vapor continuum, corresponding to 159 channels.

The forward model F is:

$$F = \rho^0_{TOA} + \Delta\rho^p_{TOA}, \tag{2}$$

where ρ^0_{TOA} is the TOA reflectance of a plume-free atmosphere, $\Delta\rho^p_{TOA}$ is the TOA reflectance variation due by the aerosol inside the plume, the subscript p is an atmosphere with a plume and the subscript 0 is a plume-free atmosphere.

$$\begin{aligned}\Delta\rho^p_{TOA} &= \rho^p_{TOA} - \rho^0_{TOA} \\ &= \left(\Delta L^p_{atm} + \rho\frac{\Delta(ET)}{\pi(1-\rho S^0)}\right) \times \frac{\pi}{E_{TOA}\mu_s},\end{aligned} \tag{3}$$

where ρ^p_{TOA} is a TOA reflectance of a plume atmosphere, ΔL^p_{atm} is the atmospheric radiance differential, $\Delta(ET)$ is the differential product of the downward solar irradiance and the atmospheric transmittance.

$$\begin{aligned}\Delta(ET) =& \Delta E^p_{dir} \times (T^0_{dir} + T^0_{sca}) \\ &+ (E^0_{dir} + E^0_{sca}) \times \Delta T^p_{dir} \\ &+ \Delta E^p_{dir} \times \Delta T^p_{dir}.\end{aligned} \tag{4}$$

We consider here that E^0_{sca} and T^0_{sca} are not modified by the plume. The atmospheric terms affected by the plume aerosols are interpolated from a Look-Up Table (LUT) of atmospheres with a plume computed with MODTRAN. The plumes are simulated at an altitude of 50 m above the ground and with a 100 m thickness [2]. The surface reflectances below the plume are computed with the Coupled Non-negative Matrix Factorization (CNMF) proposed by Yokoya et al. (2011) [3]. The CNMF is a hypersharpening method. The CNMF uses both PRISMA and MSI image data.

The aerosol optical model (sulfate or soot) and the a priori aerosol radius are prescribed for each site based on the literature [4, 5, 6]. The AOT first guess is computed with a sequential method that minimizes the difference between the measured plume aerosol signal and the MODTRAN's LUTs plume aerosol signal.

4. RESULTS AND DISCUSSIONS

Maps of AOT and aerosol modal radius in the gas flaring plume at Hassi Messaoud are presented in Figures 2. We observe that the AOT values have a physically consistent distribution in the plume. A strong AOT gradient is present just after the source. The plume is probably emitted in puffs because two local maxima of AOTs are observed at 1 km and 2 km from the source.

Figure 3 shows the aerosol radius and AOT along a longitudinal transect (dashed black line in Figure 2). The transect starts from the source and goes to the tail of the plume. The AOT decreases from a maximum of 1.02 at 250 m at the source to 0.18 at 750 m downwind. We note that the aerosol radius is at a maximum of 0.39 μm close to the source. The aerosol radius remains nearly constant beyond 550 m at around 0.15 μm until the tail of the plume.

The retrieved aerosol radii are in the same order of magnitude as literature data in the case of gas flaring site. The retrieved AOTs and aerosol radii range for the other sites is

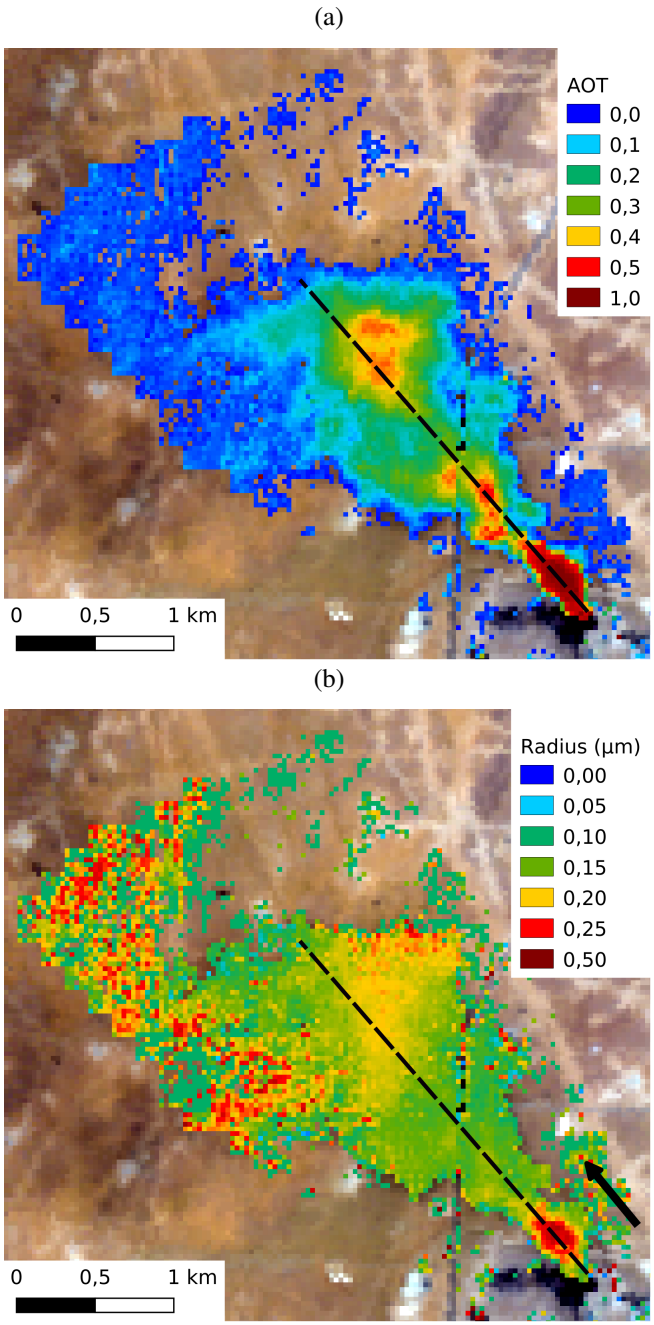

Fig. 2. Retrieval of the (a) AOT and (b) aerosol radius in the gas flaring plume observed by PRISMA at Hassi Messaoud on Sept. 7, 2021.

given in Table 1. The highest AOT are observed in the steel factory plume in Wuhan, China. The retrieved aerosol radii in the plume of the steel factory and the coal-fired power plant are higher than the ones in the gas flaring plume and also higher than literature reported values. It should be noted that we assume a single mode aerosol size distribution however the potential contribution of a coarse mode could skew the retrieval towards higher radius.

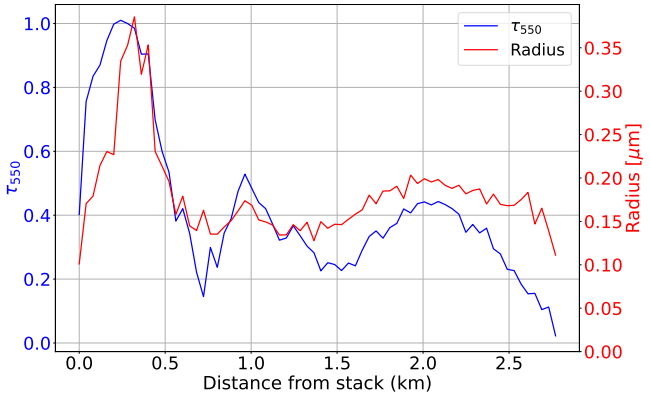

Fig. 3. Retrieved AOT and aerosol radius associated to the longitudinal transect on Figure 2.

Table 1. Amplitude of AOT (τ_{550}) and aerosol modal radius (r) retrieved in the studied industrial plumes.

Sites	τ_{550} (no unit)	r (μm)
Gas flaring	0.2 - 1.0	0.10 - 0.39
Steel plant	0.5 - 3.4	0.30 - 0.70
Coal-fired power plant	0.6 - 2.4	0.40 - 1.25

5. CONCLUSION

AOTs and aerosol modal radii were retrieved in three different types of industrial plumes located around the world. As in-situ measurements are rare or non-existent, it is complex to validate these results. However, we have shown that we are able to retrieve physically consistent AOTs values for all three sites thanks PRISMA measurments. Introducing a bimodal size distribution for the coal-fired power plant and the steel factory plumes may improve the aerosol radius estimation. The case studies demonstrate the ability of a coupled hyper/moderate spectral satellite imagery for stack plume analysis and open the way to estimate particulate flux emission from stack using space remote sensing.

Acknowledgments: This work was supported by CNES under contract named IMHYS. Gabriel Calassou's thesis is cofunded by ONERA, The French Aerospace Lab and CNES.

6. REFERENCES

[1] G. Calassou, P.-Y. Foucher, and J.-F. Léon, "Industrial plume properties retrieved by optimal estimation using combined hyperspectral and sentinel-2 data," *Remote Sensing*, vol. 13, no. 10, pp. 1865, may 2021.

[2] H. Marris, K. Deboudt, P. Augustin, P. Flament, F. Blond,

E. Fiani, M. Fourmentin, and H. Delbarre, "Fast changes in chemical composition and size distribution of fine particles during the near-field transport of industrial plumes," *Science of The Total Environment*, vol. 427-428, pp. 126–138, 2012.

[3] N. Yokoya, T. Yairi, and A. Iwasaki, "Coupled nonnegative matrix factorization unmixing for hyperspectral and multispectral data fusion," *IEEE Transactions on Geoscience and Remote Sensing*, vol. 50, no. 2, pp. 528–537, feb 2012.

[4] C. Leoni, J. Hovorka, V. Dočekalová, T. Cajthaml, and S. Marvanová, "Source impact determination using airborne and ground measurements of industrial plumes," *Environmental Science & Technology*, vol. 50, no. 18, pp. 9881–9888, 2016.

[5] M. R. Johnson, R. W. Devillers, and K. A. Thomson, "Quantitative field measurement of soot emission from a large gas flare using sky-LOSA," *Environmental Science & Technology*, vol. 45, no. 1, pp. 345–350, jan 2011.

[6] K. Saarnio, A. Frey, J. V. Niemi, H. Timonen, T. Rönkkö, P. Karjalainen, M. Vestenius, K. Teinilä, L. Pirjola, V. Niemelä, J. Keskinen, A. Häyrinen, and R. Hillamo, "Chemical composition and size of particles in emissions of a coal-fired power plant with flue gas desulfurization," *Journal of Aerosol Science*, vol. 73, pp. 14–26, jul 2014.